THE JOURNAL OF BIOLOGICAL CHEMISTRY
Vol. 278, No. 10, Issue of March 7, pp. 8586–8596, 2003
Printed in U.S.A.

Characterization of Prominin-2, a New Member of the Prominin Family of Pentaspan Membrane Glycoproteins*[S]

Received for publication, October 18, 2002, and in revised form, December 26, 2002
Published, JBC Papers in Press, January 3, 2003, DOI 10.1074/jbc.M210640200

Christine A. Fargeas‡, Mareike Florek§, Wieland B. Huttner‡¶, and Denis Corbeil‡§‖

From the ‡Max-Planck-Institute of Molecular Cell Biology and Genetics, Pfotenhauerstrasse 108 and §Medical Clinic and Polyclinic I TU-Dresden, Fetscherstrasse 74, D-01307 Dresden, Germany

Prominin/CD133 is a 115/120-kDa integral membrane glycoprotein specifically associated with plasma membrane protrusions in epithelial and non-epithelial cells including neuroepithelial and hematopoietic stem cells. Here we report the identification as well as molecular and cell biological characterization of mouse, rat, and human prominin-2, a 112-kDa glycoprotein structurally related to prominin (referred to as prominin-1). Although the amino acid identity between prominin-2 and prominin-1 is low (<30%), their genomic organization is strikingly similar, suggesting an early gene duplication event. Like prominin-1, prominin-2 exhibits a characteristic membrane topology with five transmembrane segments and two large glycosylated extracellular loops. Upon its ectopic expression in Chinese hamster ovary cells as a green fluorescent protein fusion chimera, prominin-2 was also found to be associated with plasma membrane protrusions, as revealed by its co-localization with prominin-1, suggesting a related role. Consistent with this, prominin-2 shows a similar tissue distribution to prominin-1, being highly expressed in the adult kidney and detected all along the digestive tract as well as in various other epithelial tissues. However, in contrast to prominin-1, prominin-2 was not detected in the eye, which perhaps explains why a loss-of function mutation in the human *prominin-1* gene causes retinal degeneration but no other obvious pathological signs. Finally, we present evidence for the existence of a family of pentaspan membrane proteins, the prominins, which are conserved in evolution.

Prominin-1 is a 115-kDa glycoprotein originally described to be expressed on the apical surface of mouse neuroepithelial stem cells and several other epithelia including kidney brush border membranes (1). Remarkably, within the apical plasma membrane domain, prominin-1 is selectively associated with microvilli and other related plasma membrane protrusions rather than with the planar portion of the membrane (1, 2). This specific subcellular localization does not depend on an epithelial phenotype because prominin-1 is selectively found in plasma membrane protrusions when ectopically expressed in fibroblasts (1). The retention of prominin-1 in these plasma membrane protrusions involves a novel cholesterol-based lipid microdomain, referred to as Lubrol raft, in which prominin-1 interacts specifically with cholesterol (3).

The human orthologue of mouse prominin-1 (CD133; prominin (mouse)-like 1 (PROML1)) has been originally identified as an antigenic marker (AC133 antigen) on a subset of hematopoietic stem cells (Refs. 4 and 5 and for review see Ref. 6). Human and murine prominin-1 share a similar, if not identical, cellular distribution and subcellular localization (7, 8).[1] They show an average 60% amino acid identity and display a characteristic membrane topology that is unique among the multispan transmembrane proteins, with an N-terminal extracellular domain, five transmembrane segments flanking two short cytoplasmic loops and two large glycosylated extracellular loops (over 250 residues each), and a cytoplasmic C-terminal domain (9–11).

Although the precise physiological function of prominin-1 is incompletely understood, a clue about its role comes from studying human pathology. In a consanguineous pedigree from India, individuals afflicted with retinal degeneration are homozygous carriers of a frameshift mutation in the *prominin-1* gene, which results in a truncated protein that is no longer transported to the cell surface (12). In keeping with the preferential association of prominin-1 with plasma membrane protrusions (1, 2, 7), prominin-1 is concentrated in the membrane evaginations at the base of the outer segment of rod photoreceptor cells, which are precursor structures in the biogenesis of photoreceptor disks (12). Given the ability of prominin to interact with cholesterol within a specific membrane microdomain (3), it has therefore been proposed that this pentaspan membrane protein has a role in establishing and/or maintaining certain plasma membrane protrusions (8).

The existence of several open reading frames (ORFs)[2] in the *Caenorhabditis elegans* genome encoding predicted proteins structurally related to prominin-1 (9) raised the possibility that prominin-1 may be the first characterized members of a novel family of polytopic membrane proteins occurring throughout the animal kingdom. The existence of a prominin paralogue in humans could potentially explain why the homozygous carriers of the frameshift mutation in the *prominin-1* gene resulting in

* The costs of publication of this article were defrayed in part by the payment of page charges. This article must therefore be hereby marked "*advertisement*" in accordance with 18 U.S.C. Section 1734 solely to indicate this fact.

[S] The on-line version of this article (available at http://www.jbc.org) contains additional text, Fig. 1, and Tables I–III.

The nucleotide sequence(s) reported in this paper has been submitted to the GenBank™/EBI Data Bank with accession number(s) AF508942, AF269062, AF128113, AF245303, AF245304, AF160970, AF373869, AF127935, AF197345, and AF406812.

¶ Supported by Deutsche Forschungsgemeinschaft Grants Hu 275/7-1 and Hu 275/8-1, the German-Israeli Foundation for Scientific Research and Development, and the Fonds der Chemischen Industrie. To whom correspondence may be addressed. Tel.: 49-351-210-1500; Fax: 49-351-210-1600; E-mail: HUTTNER@mpi-cbg.de.

‖ To whom correspondence may be addressed. Tel.: 49-351-210-1488; Fax: 49-351-210-1489; E-mail: CORBEIL@mpi-cbg.de.

[1] M. Florek, D. Freund, G. Ehninger, W. B. Huttner, and D. Corbeil, manuscript in preparation.

[2] The abbreviations used are: ORF, open reading frames; CHO, Chinese hamster ovary; PNGase F, peptide:*N*-glycosidase; endo H, endo-β-*N*-acetylglucosaminidase H; nt, nucleotide; GFP, green fluorescent protein; PBS, phosphate-buffered saline; mAb, monoclonal antibody.

retinal degeneration (12) lack other obvious pathological signs.

In the present study, we report the identification, molecular cloning, cell biological characterization, tissue distribution, and genomic organization of novel mouse, rat, and human cDNAs encoding a membrane glycoprotein structurally related to prominin-1 and referred to as prominin-2. Furthermore, sequence analyses of mammalian prominin-2 as well as proteins predicted from several expressed sequence tag (EST) clones derived from various other vertebrate and invertebrate organisms, such as chicken, fish, fly, and worm, provide a first description of the prominin family.

EXPERIMENTAL PROCEDURES

Data Base Searches and Computer Analyses—Nucleotide and protein sequence data bases were searched at the National Center for Biotechnology Information, Berkeley *Drosophila* Genome Project data base, and Celera Discovery System by using the BLAST network services (13). ScanProsite searches in Swiss-Prot and TREMBL protein data bases (including weekly releases of Swiss-Prot) were performed at the ExPASy Molecular Biology www server (14) of the Swiss Institute of Bioinformatics (www.expasy.ch/). The exonic organization of human and mouse *prominin-2, prominin-1,* and *Drosophila melanogaster prominin-like* genes were determined by comparing a given cDNA with the corresponding genomic sequence using BLAST. Pairwise protein sequence comparisons were performed using the ALIGN program with a BLOSUM 50 matrix (15) and multiple sequence alignments using the ClustalW program (16). Molecular phylogenetic analysis was done using PHYLIP software (17) at the infobiogen server (www.infobiogen.fr). Reliability of the branching was analyzed by the bootstrap method with 200 replications (18).

EST Clones and DNA Sequencing—The EST clones, Life Tech mouse embryonic clone mp20c10 (GenBank™ accession number AA396526) and human IMAGE clone qu80c08 (GenBank™ accession number AI285647), were obtained from Resource Center/Primary Data of the German Human Genome Project at the Max-Planck-Institute for Molecular Genetics; the human IMAGE clone qk36c08 (GenBank™ accession number AI92608), *Danio rerio* clones fb75c01 (GenBank™ accession number AI545699) and fm10h05 (GenBank™ accession number BG307062), *D. melanogaster* clones LD23965 (GenBank™ accession number AA820383), LD22538 (GenBank™ accession number AA817301), and LD16666 (GenBank™ accession number AA441662) were purchased from Research Genetics, Inc. (Huntsville, AL); the human clone au65a10 (GenBank™ accession number AI929095) and chicken clone pgf1n.pk006.j1 (GenBank™ accession number BI065967) were from Genome System Inc. (St. Louis, MO) and University of Delaware Chicken EST data base of Delaware Biotechnology Institute (Newark, DE), respectively. All EST clones were completely sequenced on both strands by primer walking along the cDNA, using either the Autoread™ sequencing kit and an ALFexpress™ sequencer (Amersham Biosciences) or the ABI PRISM™ Dye Terminator Cycle Sequencing kit and an Applied Biosystems model 377 DNA sequencer (Applied Biosystems, Foster City, CA).

Cloning of the Murine, Human, and Rat Prominin-2 cDNA Sequences—Cloning of the murine, human, and rat prominin-2 cDNA sequences is described in detail in the Supplemental Material.

Plasmid Construction—The eukaryotic expression plasmid pCMV-prominin-2, containing the entire coding sequence of mouse prominin-2, was obtained by subcloning the *Hin*dIII–*Xho*I cDNA fragment released from the pCR-Blunt II TOPO-mouse prominin-2 plasmid into pCMV-Tag5c (Stratagene) digested with the same restriction enzymes. To obtain the pCMV-mouse prominin-2-myc plasmid, an *Xho*I site, destroying the wild-type amber stop codon of the mouse prominin-2 cDNA and allowing the fusion in-frame with the Myc tag cDNA of pCMV-prominin-2, was introduced by PCR using m3 (see Supplemental Material) and the primer 5′-cggtgggttctcgagcttcagagag-3′. The PCR product was digested with *Acc*I and *Xho*I, and the resulting *Acc*I-*Xho*I cDNA fragment containing the mutated 3′ region of the mouse prominin-2 cDNA was used to replace the corresponding wild-type cDNA fragment in the pCMV-prominin-2 plasmid. The pEGFP-N1-prominin-2 plasmid, containing the entire coding sequence of rat prominin-2 fused in-frame to the N terminus of green fluorescent protein (GFP), was constructed by selective PCR amplification of the corresponding cDNA (GenBank™ accession number AF508942) using the oligonucleotides 5′-tgcttcccagaattccgaaaccatgacgcgca-3′ and 5′-tcaccttgcccggtggatcccatagcttcagg-3′ as 5′ and 3′ primers, respectively. The 5′ and 3′ primers created an *Eco*RI and *Bam*HI restriction site, respectively. In addition, the nucleotide sequence flanking the initial start codon in the 5′ primer (see underlined letters above) was converted to a Kozak consensus translation initiation site to further increase the translation efficiency. The resulting PCR fragment was digested with *Eco*RI and *Bam*HI and cloned into the corresponding sites of pEGFP-N1vector (Clontech).

The bacterial expression plasmid pGEX-E3, containing the mouse prominin-2 cDNA from nt 1891 to 2193 (residues Ile^{582}–Thr^{682}) fused in-frame to glutathione *S*-transferase, was constructed by selective PCR amplification of the corresponding cDNA using the oligonucleotides 5′-atacccacagaattcagcaggagc-3′ and 5′-gacactgaattcgagctaggtcacaagg-3′ as 5′ and 3′ primers, respectively. Both oligonucleotides created an *Eco*RI restriction site, and the 3′ primer introduced in addition an amber stop codon. The resulting PCR fragment was digested with *Eco*RI and cloned into the corresponding site of pGEX-2T vector (Amersham Biosciences).

In all cases, the PCR DNA fragments were verified by sequencing.

Antiserum against Recombinant Prominin-2—The recombinant glutathione *S*-transferase-prominin-2 fusion protein, containing a fragment of the second extracellular loop of prominin-2 (residues Ile^{582}–Thr^{682}), was expressed in BL21 *Escherichia coli*, purified on glutathione-Sepharose 4B beads (Amersham Biosciences) as described previously (2), and used as antigen to generate the rabbit antiserum αE3 (alias SA7564) (EUROGENTEC Bel S.A. Seraing, Belgium).

Cell Culture and Transfection—CHO cells were cultured as described previously (7) and either double-transfected with the eukaryotic expression plasmid pRc/CMV-prominin containing the mouse prominin-1 cDNA (1) and the pEGFP-N1-prominin-2 plasmid, or transfected with the pCMV-mouse-prominin-2 plasmid or the pCMV-mouse prominin-2-myc plasmid alone, using LipofectAMINE (Invitrogen) according to the supplier's instructions. After 24 h, the medium was changed, and the cells were incubated for an additional 17 h in the presence of 5 mM sodium butyrate. Transiently transfected cells were then either used for immunofluorescence or solubilized in ice-cold solubilization buffer (1% Triton X-100, 0.1% SDS, 150 mM NaCl, 5 mM EGTA, 50 mM Tris-HCl, pH 7.5, 1 mM phenylmethylsulfonyl fluoride, 2 μg/ml leupeptin, 10 μg/ml aprotinin), and the detergent extract obtained after centrifugation (10 min, 10,000 × *g*) was used for deglycosylation, SDS-PAGE, and immunoblotting.

Endoglycosidase Digestions and Immunoblotting—CHO cell detergent extracts corresponding to one-fifth of an 80% confluent 60-mm dish, membranes from adult mouse kidney (50 μg of protein) (11), or detergent extracts (100 μg protein) corresponding to one-eighth of an adult mouse eye prepared as described (12) were incubated overnight at 37 °C in the absence or presence of either 1 unit of peptide:*N*-glycosidase F (PNGase F) or 10 milliunits of endo-β-*N*-acetylglucosaminidase H (endo H) according to the manufacturer's instructions (Roche Molecular Biochemicals). Proteins were then analyzed by SDS-PAGE and transferred to poly(vinylidene difluoride) membranes (Millipore Corp. Bedford, MA; pore size 0.45 μm) using a semi-dry transfer cell system (Cti, Idstein, Germany). After the transfer, membranes were incubated overnight at 4 °C in blocking buffer (PBS containing 5% low fat milk powder and 0.3% Tween 20). Prominin-2 was then detected using αE3 antiserum (1/3000) followed by horseradish peroxidase-conjugated secondary antibody, both diluted in blocking buffer. Antigen-antibody complexes were visualized using enhanced chemiluminescence (ECL system, Amersham Biosciences).

Immunofluorescence and Confocal Microscopy—Cell surface immunofluorescence analysis was carried out as described previously (2). Prominin-1 and/or prominin-2-GFP transfected CHO cells grown on glass coverslips were washed with Ca/Mg-PBS (PBS containing 1 mM $CaCl_2$ and 0.5 mM $MgCl_2$), first at room temperature and then on ice, and surface-labeled for 30 min at 4 °C by the addition of the rat mAb 13A4 (10 μg/ml) against prominin-1 (1) or mouse mAb anti-GFP (clones 7.1 and 13.1; 1/500) (Roche Molecular Biochemicals) diluted in immunofluorescence buffer (Ca/Mg-PBS containing 0.2% gelatin). Unbound antibodies were removed by five washes with ice-cold immunofluorescence buffer. Fixative, 3% paraformaldehyde in PBS, was added to the cells on ice, and the coverslips were placed at room temperature for 30 min. The fixative was removed by three washes with immunofluorescence buffer, and the residual formaldehyde was quenched for 30 min with 0.1 M glycine in PBS. The cells were then incubated for 30 min at room temperature with Cy3-conjugated goat anti-rat IgG (H + L) or rhodamine Red-X conjugated goat anti-mouse IgG (H + L) (Jackson ImmunoResearch). Coverslips were rinsed sequentially with immunofluorescence buffer, PBS, and distilled water, and mounted in Mowiol 4.88 (Calbiochem).

In experiments with fixed, permeabilized cells, prominin-2, prominin-2-myc, or prominin-2-GFP transfected CHO cells grown on glass

coverslips were washed with PBS and fixed with 3% paraformaldehyde in PBS for 30 min at room temperature. Coverslips were then rinsed with, and incubated for 10 min in, PBS containing 50 mM ammonium chloride. In the case of prominin-2-GFP transfected cells, the fixed cells were permeabilized and blocked with 0.2% saponin, 0.2% gelatin in PBS (blocking solution) for 30 min at room temperature. Cells were then incubated sequentially for 30 min at room temperature with mouse mAb anti-GFP (1/500) and rhodamine Red-X conjugated goat anti-mouse IgG (H + L), both in blocking solution. Coverslips were rinsed and mounted as described above. In the case of prominin-2 or prominin-2-myc transfected cells, the fixed cells were incubated sequentially with 0.2% gelatin in PBS for 30 min, PNGase F buffer (0.1% Triton X-100, 0.05% SDS, 25 mM EDTA, 50 mM sodium phosphate, pH 7.2, and 1% β-mercaptoethanol) containing 1 unit of PNGase F for 3 h, and 0.2% gelatin in PBS for 30 min, all at room temperature. Cells were then double-labeled for 30 min at room temperature with αE3 antiserum (1/500) and mouse mAb anti-c-Myc antibody (clone 9E10; 1/100) (Sigma) followed by Cy3-conjugated goat anti-rabbit IgG (H + L) and Cy2-conjugated goat anti-mouse IgG (H + L) (Jackson ImmunoResearch), all diluted in PBS containing 0.2% gelatin. Coverslips were rinsed and mounted as described above.

The cells were observed with a Leica TCS SP2 confocal laser scanning microscope using a $\times$100/1.40–0.7 objective. The confocal settings were such that the photomultipliers were within their linear range. With prominin-1 and prominin-2-GFP double-transfected cells, the GFP and Cy3 fluorophore were excited sequentially to minimize potential of cross-collection of signal. The images shown were prepared from the confocal data files using Adobe Photoshop software.

mRNA Expression Analysis—Northern blot analyses were performed using either mouse Northern blot membrane (Clontech, catalogue number 7762-1) or human Northern blot membranes (Clontech, catalogue numbers 7780-1 and 7782-1). Blots 7782-1 and 7780-1/7762-1 contain ~1 and 2 μg of poly(A)$^+$ RNA per lane, respectively.

A *Bst*EII-digested PCR fragment corresponding to nt 1880–2634 of the murine prominin-2 cDNA (GenBank™ accession number AF269062) and an *Eco*RV-*Bst*EII fragment (nt 1852–2617) derived from the 5.0-kb human prominin-2 cDNA (GenBank™ accession number AF245303) were used to generate the murine and human prominin-2-specific cDNA probes, respectively. For the selective PCR amplification of the murine probe, the sense m6 (5′-atacccacagaattcagcaggagc-3′) and antisense m7 (5′-gtcatgaggagaaagtgc-3′) primers were used together with the murine EST clone mp20c10 as template (see Supplemental Material). The PCR product was digested with *Bst*EII, and the resulting 755-bp fragment was purified on an agarose gel. The human prominin-1 probe has been described previously (7).

Probes were labeled with [α-^{32}P]dCTP by the random-prime method using the Rediprime kit (Amersham Biosciences). In all cases, blots were prehybridized at 68 °C for 30 min and incubated with the appropriate radiolabeled probe at 68 °C for 1 h in the Expresshyb™ hybridization solution (Clontech). After hybridization, blots were washed at room temperature with solution 1 (2× SSC, 0.05% SDS), followed by solution 2 (0.1× SSC, 0.1% SDS) at 50 °C according to the Clontech protocol (manual PT1190-1). Blots were analyzed by autoradiography at −80 °C using Kodak X-Omat AR x-ray film and an intensifying screen (3 and 7 days of exposure). The blots were then stripped and, before a new hybridization, re-exposed for 3 days to ascertain the complete removal of the radioactive probe.

Northern dot blot analysis was performed using Human Multiple Tissue Expression (MTE™) Array membrane (Clontech, catalogue number 7775-1). The amount of poly(A)$^+$ RNA in each dot of the array was normalized by the manufacturer to yield similar hybridization signal for eight housekeeping genes. Therefore, the amounts of mRNA in each dot vary from 50 to 956 ng, and the array allows for comparative analysis of gene expression in various tissues. The blot was hybridized with the human prominin-2-radiolabeled probe for 6 h at 65 °C and washed according to the Clontech protocol (manual PT3307-1). The blot was exposed for 2 days at −80 °C. For quantification, non-saturated exposures were scanned with an ARCUS II scanner and quantified using MacBas software (Raytest Isotopenmessgeräte GmbH, Pforzheim, Germany).

RESULTS

Identification and Molecular Cloning of Prominin-2—To identify potential vertebrate paralogues of prominin-1, data bases were searched with human and mouse prominin-1 sequences, and EST clones showing homology were sequenced and used to obtain full-length cDNAs by PCR amplification. This eventually resulted in the identification and molecular cloning of human, mouse, and rat prominin-2, as described in detail in the Supplemental Material.

Prominin-2 Is Structurally Related to Prominin-1—The ORF of human and rat prominin-2 cDNAs predicts an 834-amino acid protein with a molecular weight of 91,900 and 92,800, respectively, whereas that of mouse prominin-2 cDNA predicts an 835-amino acid protein with a molecular weight of 93,200 (Fig. 1). For all three prominin-2 sequences, hydropathy analysis indicates six hydrophobic segments (data not shown). The first N-terminal hydrophobic segment most likely corresponds to a signal peptide. A potential signal peptidase cleavage site is found after serine 21 (Fig. 1, *triangle*). The other five hydrophobic segments constitute putative transmembrane domains (Fig. 1, *solid lines*). Strikingly, the similarity of the hydropathy profiles of prominin-2 and prominin-1 proteins suggests the same membrane topology. Consequently, human and rodent prominin-2, like prominin-1, are predicted to be pentaspan membrane proteins with two large extracellular loops, each containing more than 250 residues. Like prominin-1, prominin-2 contains a cysteine-rich region of as yet unknown function, which is located at the transition of the first transmembrane segment to the first small cytoplasmic loop (residues 128–136) (Fig. 1, *asterisks*). In all three prominin-2 sequences, the up to nine potential *N*-glycosylation sites are found in the two extracellular loops (data not shown), with six conserved in position, two in the first and four in the second loop (Fig. 1, $\vee$). The two large extracellular loops also contain six cysteine residues conserved in position between prominin-2 and prominin-1 that are likely to form disulfide bridges (Fig. 1, #).

The predicted primary structures of mouse and rat prominin-2 are highly related to each other, with an overall amino acid identity and similarity of 88 and 93%, respectively. Human and rodent prominin-2 show ≈75% overall amino acid identity. Remarkably, the C-terminal domain, constituted in all three molecules by the last 34 residues, is perfectly conserved. (The lack of conservation of the C-terminal domain in the rat prominin-2 sequence reported by Zhang *et al.* (19), *i.e.* after our deposition of the first prominin-2 sequences in the data base in 2000 (8), is due to a sequence error; see Supplemental Material). Besides the C-terminal tail, the best conserved regions of human and rodent prominin-2 are the first (residues 106–127) and fifth (residues 782–801) transmembrane domains, with 91 and 95% amino acid identity, respectively. Human, mouse, and rat prominin-2 show only 26, 29, and 30% amino acid identity, respectively, to their prominin-1 paralogues.

To corroborate further that prominin-2 has the same membrane topology as prominin-1 and, specifically, that its C-terminal domain is located in the cytoplasm, prominin-2 was expressed in CHO cells as a fusion protein, with GFP tagged to its C-terminal domain. By using an antibody against GFP as topological probe in immunofluorescence experiments on either intact (Fig. 2, *A* and *B*) or saponin-permeabilized (Fig. 2, *C* and *D*) prominin-2-GFP-transfected CHO cells, we could show that the GFP tag of the fusion protein was indeed located inside the cells (Fig. 2, *B versus D*), consistent with a cytoplasmic location of the C-terminal domain of prominin-2. Similar results were obtained with C-terminally Myc-tagged prominin-2 (data not shown), further supporting a prominin-1-like membrane topology of prominin-2.

Prominin-2 Is a Plasma Membrane Glycoprotein—To analyze further the expression of prominin-2, a rabbit antiserum, referred to as αE3, was raised against a portion of the second large extracellular loop of murine prominin-2 (amino acids 582–682). Although this antiserum, upon cell surface immuno-

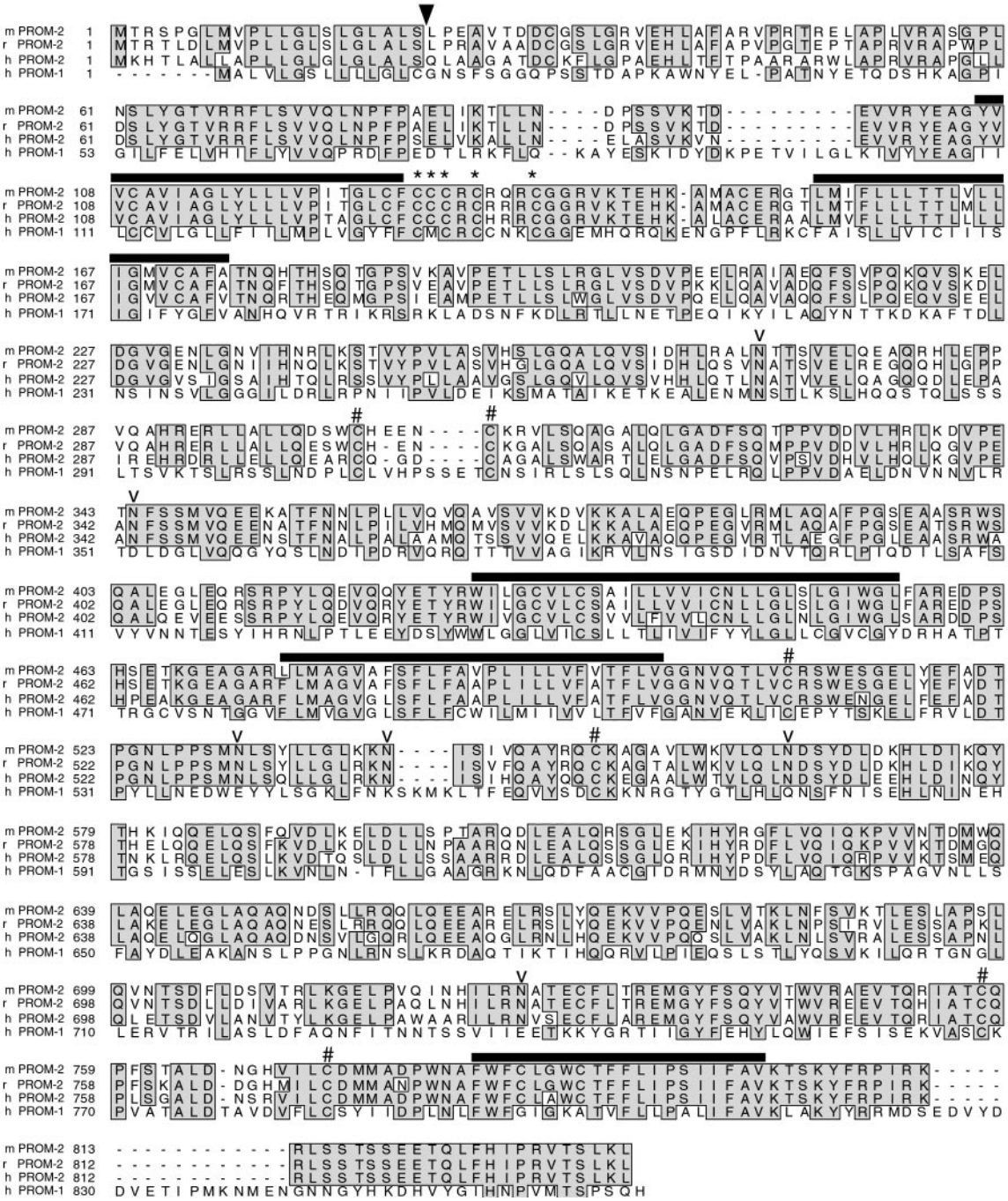

FIG. 1. **Comparison of the amino acid sequence of rodent and human prominin-2 with human prominin-1.** The mouse (*m*), rat (*r*), and human (*h*) prominin-2 (*PROM-2*) sequences determined in the present study were aligned with human prominin-1 (*PROM-1*). *Shaded boxes*, amino acid residues that are identical between at least three of the sequences; *triangle*, predicted cleavage site of the signal peptide of prominin-2; *solid lines*, predicted membrane-spanning segments; *asterisks*, cysteine-rich region; ∨, conserved potential *N*-glycosylation sites in prominin-2; #, conserved cysteine residues in the extracellular domains of prominin-2 and prominin-1.

fluorescence of transfected CHO cells, did not recognize the native form of prominin-2 (data not shown), it did reveal, upon treatment of fixed cells with PNGase F, the presence of prominin-2 at the plasma membrane (Fig. 3*A*). The authenticity of this immunostaining was confirmed by its dependence on the presence of prominin-2 cDNA upon transfection of CHO cells (Fig. 3, *A versus B*) and by the essentially identical pattern observed with the αE3 antiserum and anti-Myc antibodies upon immunostaining of CHO cells transfected with Myc-tagged prominin-2 (Fig. 3, *C* and *D*).

In CHO cells transiently transfected with the full-length mouse prominin-2 cDNA, immunoblotting with αE3 antiserum revealed two bands with apparent molecular mass of ≈112 and ≈95 kDa (Fig. 4, *top* and *bottom panels*, *lane 3*, *arrowheads* and *asterisks*, respectively). No immunoreactivity was detected when CHO cells were transfected with the expression vector alone (Fig. 4, *top* and *bottom panels*, *lane 5*). The two-band pattern of prominin-2 was reminiscent of that of prominin-1 ectopically expressed in CHO cells (1, 12) and Madin-Darby canine kidney cells (2, 3). The 95-kDa form of prominin-2 was sensitive to digestion with endo H (Fig. 4, *bottom panel*, lane 3, *asterisk*, and *lane 4*, *arrow*) and therefore represented the high mannose form localized in the endoplasmic reticulum and/or an early Golgi compartment. The 112-kDa form of prominin-2 was

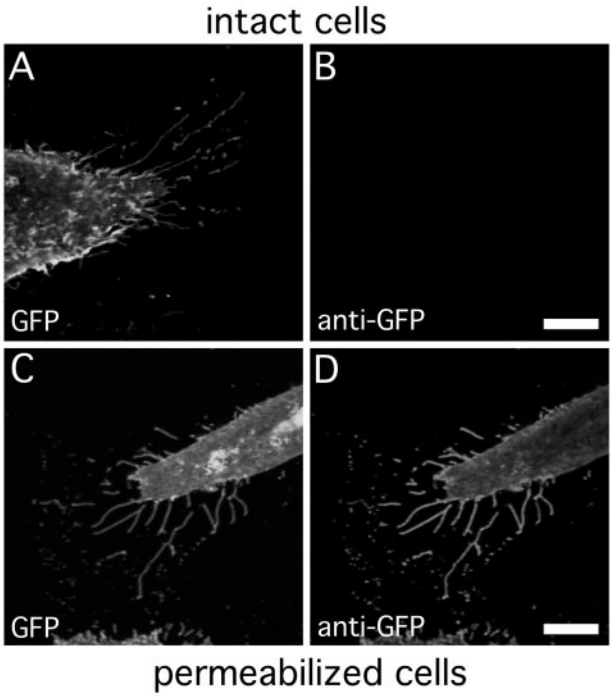

FIG. 2. **Intracellular localization of the C-terminal domain of prominin-2.** CHO cells were transiently transfected with the expression vector containing the rat prominin-2-GFP fusion protein cDNA. Intact cells at 4 °C (*A* and *B*) or paraformaldehyde-fixed, saponin-permeabilized cells (*C* and *D*) were incubated with anti-GFP antibodies (anti-GFP) followed by rhodamine Red-X conjugated goat anti-mouse antibody and double fluorescence analysis using confocal microscopy. GFP fluorescence of prominin-2-GFP fusion protein is shown in *A* and *C*. Single optical *xy* plane sections near the bottom of the cell are shown. *Bar* in *B*, 5.4 μm; *bar* in *D*, 6.2 μm.

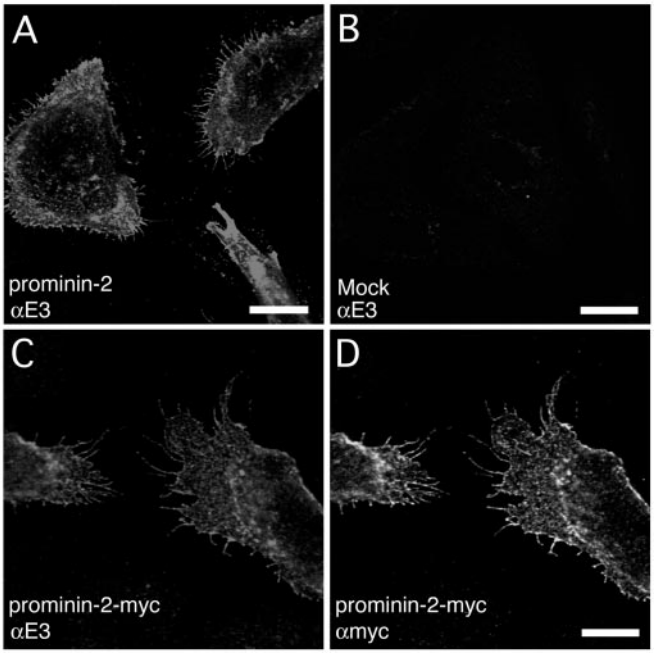

FIG. 3. **αE3 antiserum recognizes the authentic mouse prominin-2.** CHO cells were transiently transfected with the expression vector containing the mouse prominin-2 cDNA (*A*), mouse prominin-2-myc cDNA (*C* and *D*), or, as a control, vector DNA alone (*B*). Paraformaldehyde-fixed, PNGase F-treated cells were double-labeled with αE3 antiserum (*A–C*) and anti-c-Myc antibody (*D*) followed by appropriate Cy3- and Cy2-conjugated secondary antibodies and double immunofluorescence analysis using confocal microscopy. Single optical *xy* plane sections near the bottom of the cell are shown. *Bar* in *A*, 11.5 μm; *bar* in *B*, 14 μm; *bar* in *D*, 7.8 μm.

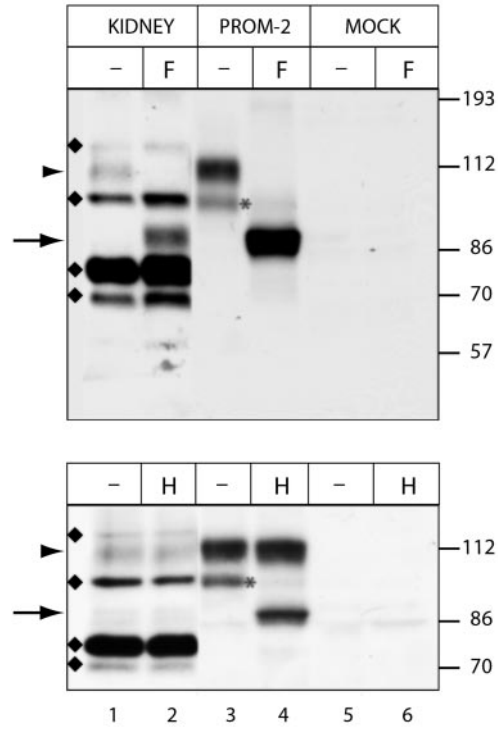

FIG. 4. **Expression of prominin-2 in CHO cells and murine kidney.** CHO cells were transiently transfected with either the expression vector containing the mouse prominin-2 cDNA (*PROM-2*) or, as a control, vector DNA alone (*MOCK*). Lysates from the CHO cells and, for comparison, from adult mouse kidney membranes (*KIDNEY*) were incubated in the absence (−) or presence of 1 unit of PNGase F (*F*, *top panel*) or 10 milliunits of endo H (*H*, *bottom panel*) and analyzed by immunoblotting with αE3 antiserum. *Arrowheads*, PNGase F-sensitive, endo H-resistant form of prominin-2; *asterisks*, PNGase F- and endo H-sensitive form; *arrows*, product after *N*-deglycosylation; *diamonds*, PNGase F- and endo H-insensitive, immunoreactive bands of unknown identity. The position of prestained apparent molecular mass markers (in kDa) is indicated on the *right*.

resistant to the endo H (Fig. 4, *bottom panel*, *lanes 3* and *4*, *arrowhead*), indicating that it had passed through the Golgi apparatus. PNGase F treatment converted both the 112- and 95-kDa forms of recombinant prominin-2 found in transfected CHO cells into an ≈88-kDa product (Fig. 4, *top panel*, *lane 4*, *arrow*), which is in agreement with the predicted molecular weight (92,100) of unglycosylated prominin-2 after cleavage of its signal peptide. PNGase F digestion also resulted in a ≈2-fold increase in prominin-2 immunoreactivity detected after immunoblotting, suggesting that complex *N*-glycans masked a significant proportion of the epitopes recognized by the αE3 antiserum. This is consistent with our observation that upon immunofluorescence analysis of prominin-2-transfected CHO cells using αE3 antiserum, plasma membrane staining for prominin-2 was only observed if the fixed cells were treated with PNGase F prior to addition of the antibody (see above, Fig. 3). Taken together, the immunofluorescence data (Fig. 3) and the immunoblotting data (Fig. 4, *lanes 3–6*) obtained with prominin-2-transfected CHO cells show that the αE3 antibody is specific for prominin-2, at least in these cells.

Surprisingly, upon immunoblotting of mouse kidney membranes using the αE3 antiserum, the pattern of immunoreactive bands was more complex. First, we observed four immunoreactive bands that showed no change in electrophoretic mobility upon PNGase F and endo H digestions (Fig. 4, *top* and *bottom panels, lanes 1* and *2*, *diamonds*) and presumably were unglycosylated proteins. The identity of these bands and their possible relationship to prominin-2 has not been investigated

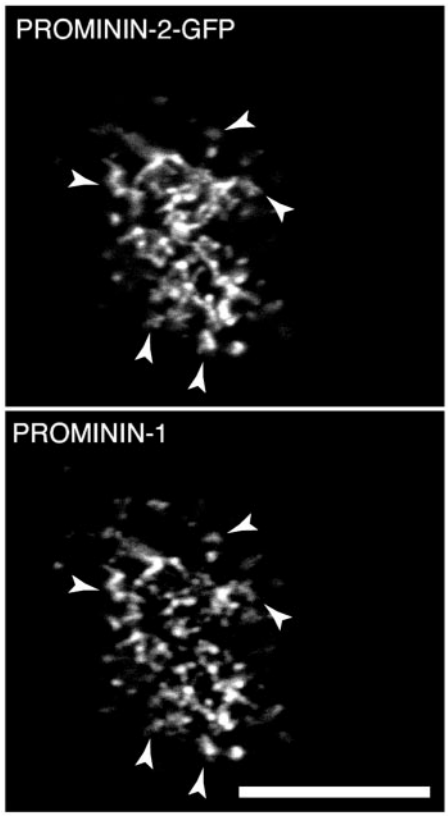

FIG. 5. **Co-localization of prominin-1 and prominin-2 in plasma membrane protrusions.** CHO cells were transiently double-transfected with the expression vectors containing either the rat prominin-2-GFP fusion protein cDNA or mouse prominin-1 cDNA, cell surface-labeled with rat mAb 13A4 against prominin-1 followed by Cy3-conjugated anti-rat antibody, and examined for the fluorescent signal of prominin-2-GFP fusion protein (*top*) and immunostaining of prominin-1 (*bottom*). Single optical *xy* plane section at the apex of the cell is shown. *Arrowheads* indicate co-localization of prominin-2 and prominin-1. *Bar*, 8 μm.

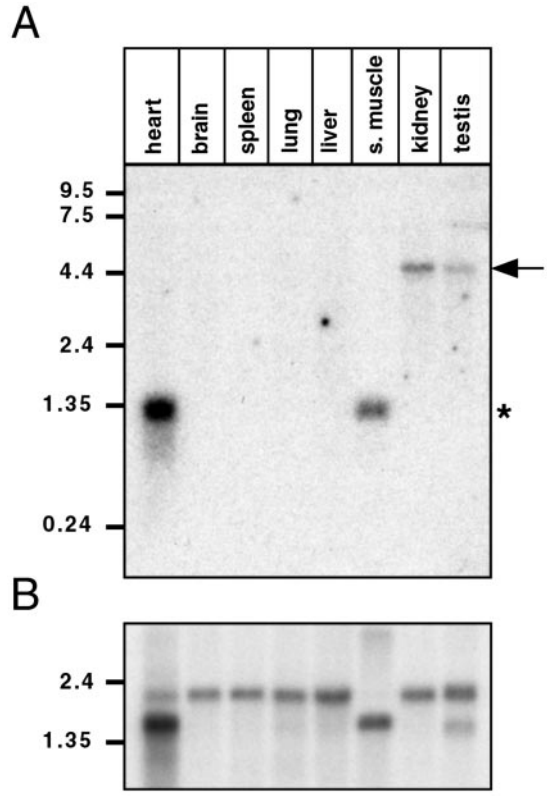

FIG. 6. **Northern blot analysis of mouse prominin-2 expression.** *A* and *B*, mouse multiple tissue Northern blot membrane was probed with mouse prominin-2 cDNA (*A*) or actin cDNA (*B*). *Arrow*, transcripts in kidney and testis; *asterisk*, transcripts in heart and skeletal muscle.

further in the present study. Second, we observed a 112-kDa band that showed the same endo H resistance (Fig. 4, *bottom panel*, *lanes 1* and *2*, *arrowhead*) and PNGase F sensitivity (Fig. 4, *top panel*, *lane 1*, *arrowhead* and *lane 2*, *arrow*) as authentic prominin-2 expressed in CHO cells. This establishes that prominin-2 is endogenously expressed in the kidney *in vivo*. Furthermore, given that all potential *N*-glycosylation sites of prominin-2 are found in the two large loops, our results also indicate that these loops are indeed located extracellularly and, hence, that prominin-2 displays the same membrane topology as prominin-1.

Co-localization of Prominin-2 with Prominin-1 in Plasma Membrane Protrusions—Because prominin-1 is specifically localized in microvilli and related plasma membrane protrusions in various cell types, it was of interest to investigate if prominin-2 is also associated with plasma membrane protrusions. To this end, we co-expressed prominin-1 and prominin-2-GFP in CHO cells and examined their potential co-localization in plasma membrane protrusions by confocal laser scanning microscopy. The pattern of green fluorescence of the prominin-2-GFP fusion protein (Fig. 5, *top panel*) largely coincided with that of prominin-1 immunofluorescence (Fig. 5, *bottom panel*), indicating the specific association of prominin-2-GFP with plasma membrane protrusions.

Tissue Distribution of Murine and Human Prominin-2 mRNAs—We examined the expression of prominin-2 mRNA in different mouse tissues by Northern blot analysis. A 4.4-kb-long transcript was found in kidney and testis (Fig. 6*A*, *arrow*), whereas a shorter transcript of 1.35 kb was detected in heart and skeletal muscle (Fig. 6*A*, *asterisk*). The length of the long transcript corresponded to what would be expected for a prominin-2 mRNA as deduced from the cDNA sequences (4307 nt). The nature of the 1.35-kb transcript, which is too short to encode full-length prominin-2, was not investigated further, also because no such transcript was detected in human tissues (see below).

As to human prominin-2, we first examined the relative abundance of its mRNA in 76 different human tissues and tumor cell lines using a multiple tissue expression array (Fig. 7*A*). Human prominin-2 showed strong expression in the adult kidney (*A7*). Prominin-2 mRNAs were also detected in all tissues of the digestive tract (*columns 5* and *6*, *A–C*), prostate (*E8*), trachea (*H7*), salivary gland (*E9*), thyroid gland (*D9*), mammary gland (*F9*), and placenta (*B8*). No expression was evident in any of the eight tumor cell lines (*column 10*), although two EST clones encoding part of human prominin-2 that derived from a colon adenocarcinoma have been deposited in the GenBank™ data base (accession numbers BE867546 and AI792608), and other EST clones (accession numbers AW292801 and BE762637) indicate that prominin-2 can be expressed in tumors of the lung and nervous system.

To characterize further human prominin-2 transcripts, Northern blot analyses were performed on poly(A)$^+$ RNA. Consistent with the two cDNAs that were amplified by PCR (Supplemental Material, Fig. 1*B*), two main transcripts of ≈5.0 and ≈4.2 kb (Fig. 7, *B* and *D*, *solid arrows*) were detected in kidney and placenta (Fig. 7*B*) and at variable levels along the digestive tract (Fig. 7*D*), whereas in the liver, a 1.5-kb transcript (too short to encode full-length prominin-2) was detected (Fig. 7, *B* and *D*, *asterisk*). The results of the dot blot analysis (Fig. 7*A*) were therefore confirmed. With longer time of exposure, a

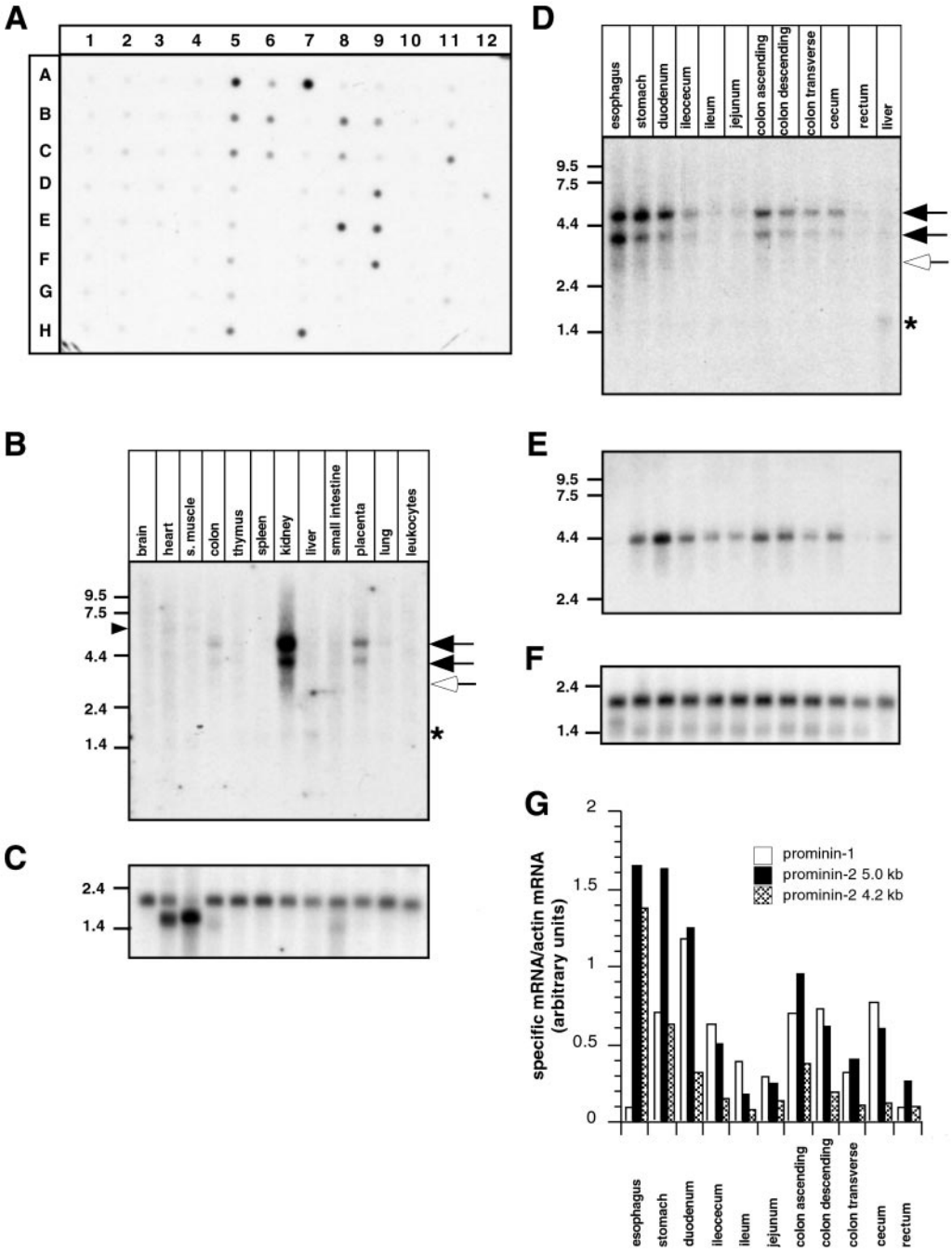

FIG. 7. **Tissue distribution of human prominin-2 mRNA.** *A*, human multiple tissue expression array membrane was probed with human prominin-2 cDNA. The various dots represent the following: *A1*, whole brain; *B1*, cerebral cortex; *C1*, frontal lobe; *D1*, parietal lobe; *E1*, occipital lobe; *F1*, temporal lobe; *G1*, paracentral gyrus of cerebral cortex; *H1*, pons; *A2*, cerebellum left; *B2*, cerebellum right; *C2*, corpus callosum; *D2*, amygdala; *E2*, caudate nucleus; *F2*, hippocampus; *G2*, medulla oblongata; *H2*, putamen; *A3*, substantia nigra; *B3*, nucleus accumbens; *C3*, thalamus; *D3*, pituitary gland; *E3*, spinal cord; *A4*, heart; *B4*, aorta; *C4*, atrium left; *D4*, atrium right; *E4*, ventricle left; *F4*, ventricle right; *G4*, interventricular septum; *H4*, apex of the heart; *A5*, esophagus; *B5*, stomach; *C5*, duodenum; *D5*, jejunum; *E5*, ileum; *F5*, ileocecum; *G5*, appendix; *H5*, colon ascending; *A6*, colon transverse; *B6*, colon descending; *C6*, rectum; *A7*, kidney; *B7*, skeletal muscle; *C7*, spleen; *D7*, thymus; *E7*, peripheral blood leukocytes; *F7*, lymph node; *G7*, bone marrow; *H7*, trachea; *A8*, lung; *B8*, placenta; *C8*, bladder; *D8*, uterus; *E8*, prostate; *F8*, testis; *G8*, ovary; *A9*, liver; *B9*, pancreas; *C9*, adrenal gland; *D9*, thyroid gland; *E9*, salivary gland; *F9*, mammary gland; *A10*, promyelocytic leukemia HL-60; *B10*, HeLa S3; *C10*, chronic myelogenous leukemia K-562; *D10*, lymphoblastic leukemia MOLT-4; *E10*, Burkitt's lymphoma, Raji; *F10*, Burkitt's lymphoma, Daudi; *G10*, colorectal adenocarcinoma, SW480; *H10*, lung carcinoma, A549; *A11*, fetal brain; *B11*, fetal heart; *C11*, fetal kidney; *D11*, fetal liver; *E11*, fetal spleen; *F11*, fetal thymus; *G11*, fetal lung; *A12*, yeast total RNA; *B12*, yeast tRNA; *C12*, *E. coli* rRNA; *D12*, *E. coli* DNA; *E12*, poly(rA); *F12*, human C_0t-1 DNA; *G12*, human DNA 100 ng; *H12*, human DNA 500 ng. *B* and *C*, human multiple tissue Northern blot membrane was probed with human prominin-2 cDNA (*B*) or actin cDNA (*C*). *D–F*, human digestive tract Northern blot membrane was probed with human prominin-2 cDNA (*D*), human prominin-1 cDNA (*E*), or actin cDNA (*F*). *B* and *D*, *solid arrows*, major transcripts; *open arrows*, *arrowhead* and *asterisks*, minor transcripts. *G*, the data obtained from Northern blot analysis of prominin-1 (*E*) and prominin-2 (*D*, *solid arrow*; upper (5.0 kb) and lower (4.2 kb)) transcripts were quantified by densitometric scanning, normalized with respect to actin mRNA (*F*) in each tissue sample, and expressed as ratio of mRNA signal.

≈3.2-kb transcript appeared in kidney, placenta, colon, and esophagus (Fig. 7, *B* and *D*, *open arrow*), a ≈6.0-kb transcript in heart and skeletal muscle (Fig. 7*B*, *arrowhead*), and a ≈5-kb transcript in the lung (data not shown). With respect to the expression of prominin-2 in the human digestive tract, the amount of the two main transcripts (5.0–4.2 kb, Fig. 7*D*, *solid*

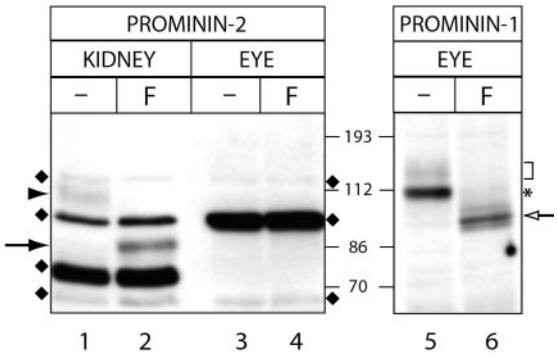

FIG. 8. **Prominin-2 is not expressed in the adult mouse eye.** Lysates from adult mouse eyes (*EYE*) and, for comparison, adult mouse kidney membranes (*KIDNEY*) were incubated in the absence (−) or presence of 1 unit of PNGase F (*F*) and analyzed by immunoblotting with either αE3 antiserum against prominin-2 (*left panel*) or mAb 13A4 against prominin-1 (*right panel*). *Left panel*, *arrowhead*, prominin-2; *arrow*, *N*-deglycosylated form of prominin-2; *diamonds*, PNGase F-insensitive immunoreactive bands of unknown identity. *Right panel*, *bracket*, PNGase F-sensitive, endo H-resistant form of prominin-1 in the eye (12); *asterisk*, PNGase F- and endo H-sensitive form of prominin-1 in the eye (12); *open arrow*, *N*-deglycosylated form of prominin-1. The position of apparent molecular mass markers (in kDa) is indicated. Note that although the three unidentified bands present in the eye are at least as strongly labeled as in the kidney (*diamonds*), prominin-2 (*arrowhead* and *arrow*) is detected in the kidney but not the eye, in contrast to prominin-1. No prominin-2 immunoreactivity was detected in the eye upon longer exposure of the immunoblot (not shown).

arrows) was compared with prominin-1 (Fig. 7*E*), normalized to actin mRNA levels (Fig. 7*F*), and plotted (Fig. 7*G*). The distribution of prominin-2 transcripts all along the digestive tract roughly paralleled that of prominin-1 transcript, with the esophagus being a notable exception; here the high expression of prominin-2 transcripts (Fig. 7*D*) was in contrast to the lack of prominin-1 transcript (Fig. 7*E*).

Although the cDNA probes used for the detection of human and mouse prominin-2 encompassed equivalent regions (*i.e.* the C-terminal third of the molecule), no 1.35-kb mRNA was detected in human skeletal muscle or heart (Fig. 7*B*), as opposed to the mouse (Fig. 6*A*). As for both mouse and human, the long transcripts (Figs. 6*A* and 7*B*) showed the highest expression in the kidney, and the nature of the short transcript in mouse heart and skeletal muscle is questionable. Moreover, no such signal was observed in mouse when an N-terminal probe was used (data not shown).

Expression of Prominin-1, but Not Prominin-2, in the Eye—Patients carrying a mutation in the *prominin-1* gene resulting in a truncated protein that is no longer transported to the cell surface are afflicted with retinal degeneration but do not show obvious pathological signs in other tissues expressing prominin-1 (12). This may be so because, given that prominin-2 is expressed in most of the tissues known to express prominin-1 (Fig. 7) (5, 7), prominin-2 may perhaps be able to functionally substitute for the lack of prominin-1. It was therefore of particular importance to investigate whether or not prominin-2 occurs in the retina. Prominin-2 was not detectable in immunoblots of the adult mouse eye (Fig. 8, *lanes 3* and *4*, *arrowhead* and *arrow*), in contrast to prominin-1 which was readily detectable (Fig. 8, *lanes 5* and *6*), confirming previous observations (12). As a positive control to detect prominin-2 immunoreactivity in immunoblots, kidney membranes were analyzed in parallel (Fig. 8, *lanes 1* and *2*, *arrowhead* and *arrow*), which yielded the same results as in Fig. 4. We conclude that prominin-2, in contrast to prominin-1, is not expressed in the retina.

Occurrence of Prominins throughout the Animal Kingdom—Data base searches and the sequencing of several EST clones displaying similarities to mammalian prominin-1 and prominin-2 (see Supplemental Material, Table I) indicate that related molecules exist throughout the animal kingdom. Prominin-like proteins are found in other vertebrates such as chicken (GenBank™ accession number AF406812) and fish (*D. rerio*, GenBank™ accession numbers AF160970 and AF373869). With regard to invertebrates, prominin-like proteins are found in fly (*D. melanogaster*, GenBank™ accession numbers AF127935 and AF197345) and worm (1, 9). Additional prominin-like proteins are also present in the data base as EST clones originating from various other species (*Ascaris suum*, GenBank™ accession numbers AW165790 and BG733718; *Strongylocentrotus purpuratus*, accession number AF122176). The evolutionary relationship between these proteins is displayed in Fig. 9*A*. The phylogenetic tree clearly indicates the segregation of two orthologous groups in mammals, prominin-1 and prominin-2 (Fig. 9*A*, *pink boxes*). The orthologue *versus* paralogue relationship of the chicken and fish prominin-like proteins with regard to the prominin-1 or prominin-2 group is more ambiguous. As can be seen from the greater consensus among vertebrate sequences (see Fig. 9*B*, *below*), invertebrate prominins are more distantly related (Fig. 9*A*).

A Prominin Signature—Multiple amino acid sequence alignment of mammalian prominin-1 and -2 as well as the prominin-like proteins from other species indicated that very few residues are conserved in all sequences. Several of such conserved residues cluster in a region including the end of the second extracellular loop and the fifth transmembrane domain (Fig. 9*B*). In this region, four completely conserved residues (Cys, Pro, Cys, and Trp) followed by a stretch of hydrophobic residues are found. Furthermore, a consensus core sequence C*X*P*X*(12,13)C*X*(5)(P/S)*X*(4)W*X*(2)h*X*(4)hh*X*h can be noticed, in which *X* stands for any residue; the number of *X* is indicated in parentheses; residues in parentheses indicate alternatives for a given position, and h stands for any hydrophobic residue (Fig. 9*B*). Interestingly, ScanProsite searches in Swiss-Prot and TREMBL protein data bases using this consensus core sequence identified no other protein. Because all the membrane proteins structurally related to prominin-1 and prominin-2 share this consensus core sequence, we propose to refer to it as the prominin signature.

The Prominin Genes—Running a BLAST search with the 5.0-kb human prominin-2 cDNA sequence as query identified the clone RP11-468G5 located to chromosome 2 (GenBank™ accession number AC009238) as containing the corresponding gene. Similarly, the celera clone GA_X5J8B7W49H2 (Celera Discovery System), located to mouse chromosome 2, was identified as containing the murine *prominin-2* gene. Human and mouse *prominin-2* genes contain 24 exons distributed over 16,853 and 14,492 bp, respectively (Fig. 10). All of the human *prominin-2* and all except one of the mouse *prominin-2* gene exon/intron boundaries conform to the GT-AG rule (see Supplemental Material, Table II). Introns are conserved in position and phase. In both *prominin-2* genes, exon 1 contains the translation-initiation codon and exon 23 the stop codon, with the 3′-untranslated region being almost entirely encoded by the exon 24. The two, 5.0 and 4.2 kb, human prominin-2 cDNAs result from alternative splicing due to the presence of an internal acceptor site within exon 24 (data not shown).

The exon/intron organization of *prominin-2* gene is strikingly similar to that of the *prominin-1* gene (Fig. 10), which was partially determined by Maw *et al.* (12) and completed in the present study (see Supplemental Material, Table III). The human *prominin-1* gene is composed of 27 exons distributed over more than 75 kb on chromosome 4 (locus p16.2-p12). We also determined the structure of the murine *prominin-1* gene (see Supplemental Material, Table III), which is located to chromo-

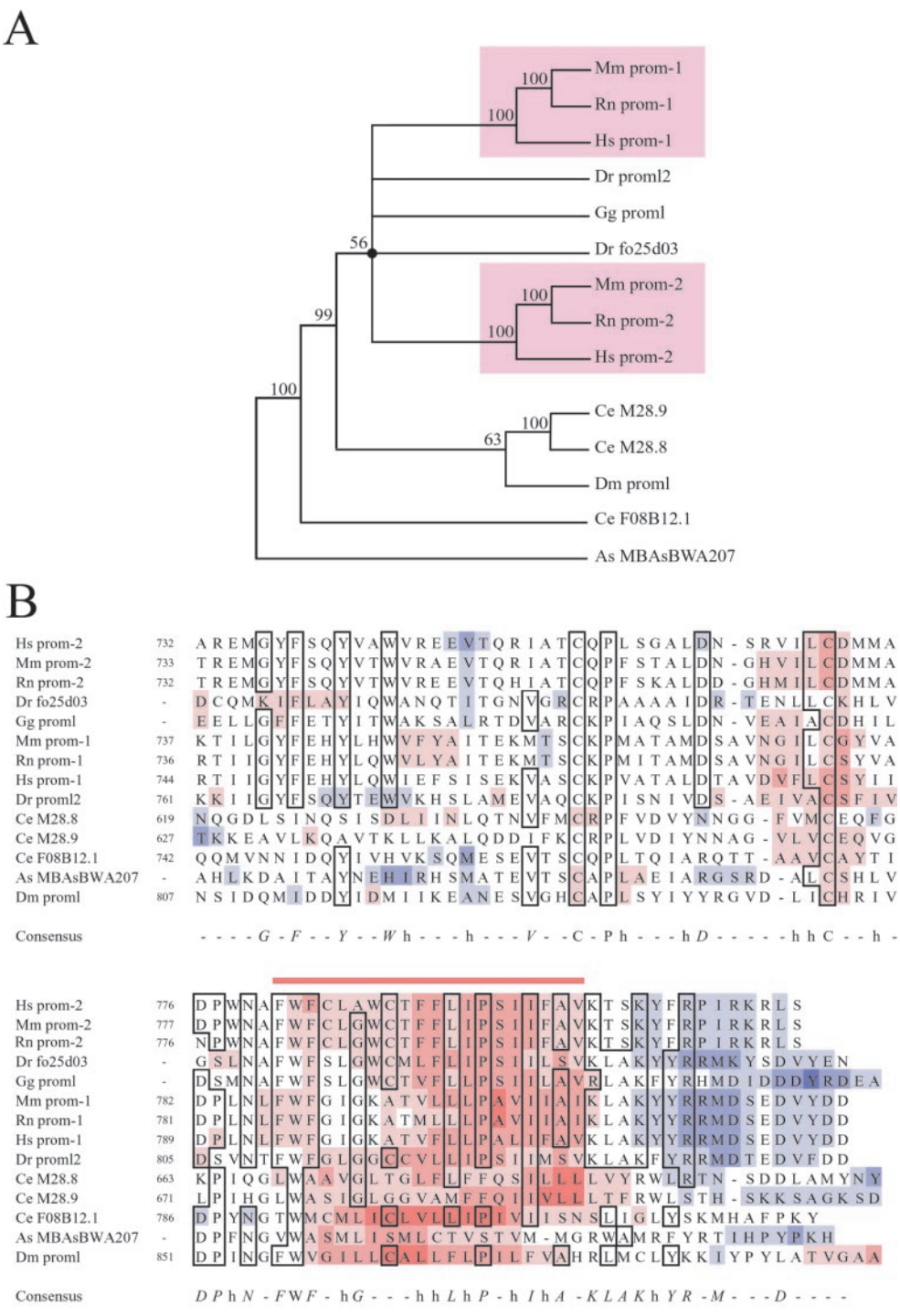

FIG. 9. **Sequence comparison of members of the prominin family.** *A*, reduced unrooted phylogenetic tree of the prominin family. The alignment in *B* was used to infer the tree by the maximum parsimony method. Bootstrap values above 50% are indicated at the nodes. Branching with bootstrap values below 50% were collapsed (*dot*). Mammalian prominin-1 and prominin-2 relatives appear in *pink boxes*. *B*, sequence alignment of prominins. The region encompassing the end of the second large extracellular loop and the fifth transmembrane domain (*red line*) of the different prominin family members were aligned using ClustalW. Sequences are displayed according to their ranking in the alignment. *Number* indicates the amino acid residues in the respective complete protein sequences. Residues identical in more than 53% of the sequences are *boxed*. *Blue* and *red* color indicate hydrophilic and hydrophobic residues (over a window of seven residues), respectively, the intensity of the color denoting the degree of hydrophilicity and hydrophobicity. In the consensus sequence, *regular uppercase letters* indicate strict (100%) consensus residues, *italic uppercase letters* preferred (>53%) residues, and *h* preferred hydrophobic residues. Abbreviations and data base accession numbers are as following *Homo sapiens* prominin-2 (*Hs prom-2*, AF245303), *Mus musculus* prominin-2 (*Mm prom-2*, AF269062), *Rattus norvegicus* prominin-2 (*Rn prom*, AF508942), *M. musculus* prominin-1 (*Mm prom-1*, AF026269), *R. norvegicus* prominin-1 (*Rn prom-1*, AF386758), *H. sapiens* prominin-1 (*Hs prom-1*, AF027208), *D. rerio* prominin-like 2 (*Dr proml2*, AF373869), *D. rerio* EST clone fo25d03 (*Dr fo25d03*, BI884488), *Gallus gallus* prominin-like (*Gg proml*, AF406812), *C. elegans* M28.8 and M28.9 (*Ce M28.8* and *Ce M28.9*, Z49911), *C. elegans* F08B12.1 (*Ce F08B12.1*, Z68104), *A. suum* EST clone MBAsBWA207 (*As MBAsBWA207*, AW165790), and *D. melanogaster* prominin-like (*Dm proml,* AF127935).

some 5 (20). As in the case of prominin-2, the structure of the mouse *prominin-1* gene turns out to be identical to that of its human orthologue. The exon/intron boundaries of prominin-1 and prominin-2 can be largely superimposed (Fig. 10). Introns, although larger in mouse and human *prominin-1* than *prominin-2*, are remarkably concordant in position and phase. In

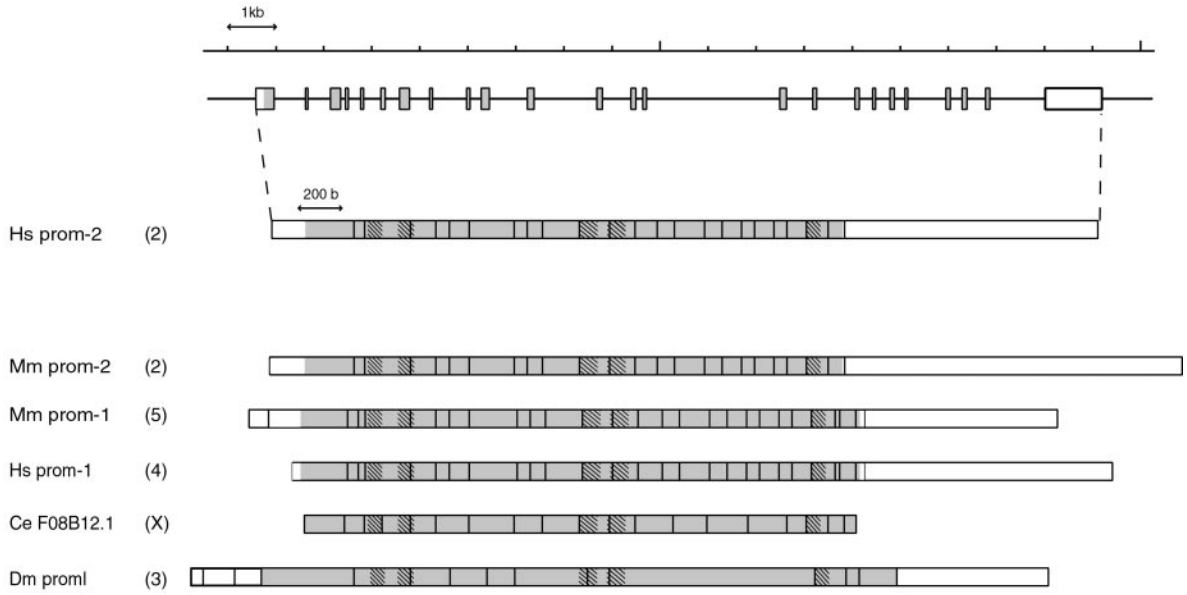

FIG. 10. **Genomic organization of human *prominin-2* and its comparison with other prominins.** The *top* of the figure shows part of the genomic clone RP11-468G5 encompassing the human prominin-2 exons, which appear as *boxes.* The corresponding human (*Hs*) prominin-2 (*prom-2*) 5.0-kb cDNA is shown below at a larger scale. Coding region appears in *gray*, and 5′- and 3′-untranslated region are in *white. Vertical lines* indicate the exon boundaries and *hatched zones* the predicted transmembrane domains. *Bottom* of figure, mouse (*Mm*) prominin-2 (*prom-2*) and prominin-1 (*prom-1*) cDNAs, human (*Hs*) prominin-1 (*prom-1*) cDNA, *C. elegans* (*Ce*) F08B12.1 predicted gene product, and *D. melanogaster* prominin-like cDNA (*Dm proml*). The chromosome carrying a given gene is indicated in *parentheses.*

comparison to the *prominin-2* genes, an additional symmetric exon (human exon 3 and mouse exon 4) encoding the 9-amino acid stretch PETVILGLK and PEIIVLALK is alternatively spliced into the N-terminal extracellular domain of human and murine prominin-1, respectively (see Refs. 10 and 21; GenBank™ accession number AK027420). Prominin-1 variants containing these additional 9 amino acid residues have been previously referred to as *B1* isoforms (8). Two other additional exons coding for part of the cytoplasmic C-terminal tail of prominin-1 are also inserted in the *prominin-1* genes (Fig. 10). Remarkably, the *prominin-2* genes are over four times more compact than the *prominin-1* genes (≈16 *versus* >75 kb).

The genomic organization of mammalian prominins also shows significant similarity with the invertebrate prominin-like proteins such as the one encoded by the *C. elegans F08B12.1* gene (22); of the 19-exon boundaries of the *F08B12.1* gene, 16 are concordant in position with the mammalian *prominin genes* (Fig. 10). Similarly, the genomic organization of *D. melanogaster* prominin-like protein (see FlyBase annotation CG7740) also exhibits several conserved exon/intron boundaries with worm and mammalian prominins (Fig. 10).

DISCUSSION

We have identified and characterized prominin-2, a novel polytopic membrane protein. Despite the low level of amino acid identity, this protein displays structural features characteristic of prominin-1, *i.e.* five transmembrane domains and two large extracellular glycosylated loops. The membrane topology of prominin-2 is supported by analyses of *N*-glycosylation and epitope accessibility. Likewise, the genomic organization of prominin-1 and prominin-2 is nearly identical, indicating that prominin-2 is indeed a paralogue of prominin-1. This is also supported by phylogenetic analysis. Identification of several prominin-like proteins in various species and the analysis of their evolutionary relationship strongly suggest that the prominin family arose through an early gene duplication event. Interestingly, whereas the prominins are conserved through metazoan evolution, they appear to be absent in yeast, suggesting that their role is related to some aspect of multicellularity.

The presence of prominin-2 in plasma membrane protrusions of transfected CHO cells, as shown by its co-localization with prominin-1, raises the possibility that prominin-2 may exert a similar function as prominin-1, which is thought to be involved in the organization of plasma membrane microdomains (8). In light of our observation that the tissue distribution of prominin-2 largely overlaps with that of prominin-1 (Fig. 7) (5, 7), this in turn would suggest that in tissues expressing both prominins, the loss of prominin-1 may be compensated by prominin-2 and vice versa. Two tissues deserve special comment in this regard, the retina and the esophagus. A mutation in the human *prominin-1* gene resulting in the loss of cell surface prominin-1 causes retinal degeneration but no obvious pathological signs in other tissues (12). If this were due to prominin-2 compensating for the loss of prominin-1 in these tissues, one would expect that prominin-2 should not be expressed in the retina, which would provide a possible explanation of the pathology observed upon the loss of cell surface prominin-1 in this tissue. Indeed, in contrast to prominin-1, prominin-2 was not detected in the eye (Fig. 8).

The opposite situation is the case for the esophagus, which expresses prominin-2 but not prominin-1. The epithelium of the esophagus is known to lack microvilli on the apical surface. Preliminary data using Madin-Darby canine kidney cells transiently transfected with prominin-2-GFP suggest that whereas prominin-1 is restricted to microvilli of the apical surface of these epithelial cells (2), prominin-2 is found not only on the apical but also the lateral plasma membrane, which also forms protrusions.[3] It therefore appears that in terms of both tissue distribution and subcellular localization, prominin-1 and prominin-2 are largely overlapping but not identical.

Both prominin-1 and prominin-2 are subject to alternative splicing. In fact, both *prominin* genes contain numerous short exons, which raises the possibility of a greater modular structure of these proteins than suggested by their domain organization derived from their pentaspan topology. Indeed, several human prominin-2 clones amplified in the present study re-

[3] M. Florek and D. Corbeil, unpublished observations.

vealed differential splicing, with variable consequences with respect to the structure of the protein. Two clones lacked exon 6, resulting in an in-frame deletion of 30 amino acids in the first large extracellular loop. Eight clones lacked the entire fifth exon, and two clones were missing part of exon 7 due to use of an alternative internal splice donor site (nucleotide 1039). The latter two deletions result in a frameshift with premature termination of the prominin-2 ORF. This would lead to the translation of short splice variants of 209 and 312 amino acid residues, respectively, with only two transmembrane domains. Given that similar observations on alternative splicing have been made with prominin-1 (8),[4,5] it appears that a wide variety of related polypeptides can be generated from the two *prominin* genes.

Acknowledgments—We thank D. Buck for the human prominin-1 cDNA; M. Maw for drawing our attention to clone NH0468G05, which contains the human *prominin-2* gene; R. Jelinek for valuable technical assistance; G. Wiebe for the excellent sequencing service; and K. Opherk for the prominin-2-GFP construct. Part of the sequencing was performed at the Sequencing Facility of the Zentrum für Molekulare Biologie of Heidelberg University. We are also grateful to Celera Discovery System and Celera Genomics for the use of their data bases. D. C. and M. F. are indebted to Prof. G. Ehninger for financial support.

REFERENCES

1. Weigmann, A., Corbeil, D., Hellwig, A., and Huttner, W. B. (1997) *Proc. Natl. Acad. Sci. U. S. A.* **94,** 12425–12430
2. Corbeil, D., Röper, K., Hannah, M. J., Hellwig, A., and Huttner, W. B. (1999) *J. Cell Sci.* **112,** 1023–1033
3. Röper, K., Corbeil, D., and Huttner, W. B. (2000) *Nat. Cell Biol.* **2,** 582–592
4. Yin, A. H., Miraglia, S., Zanjani, E. D., Almeida-Porada, G., Ogawa, M., Leary, A. G., Olweus, J., Kearney, J., and Buck, D. W. (1997) *Blood* **90,** 5002–5012
5. Miraglia, S., Godfrey, W., Yin, A. H., Atkins, K., Warnke, R., Holden, J. T., Bray, R. A., Waller, E. K., and Buck, D. W. (1997) *Blood* **90,** 5013–5021
6. Bhathia, M. (2001) *Leukemia* (*Baltimore*) **15,** 1685–1688
7. Corbeil, D., Röper, K., Hellwig, A., Tavian, M., Miraglia, S., Watt, S. M., Simmons, P. J., Peault, B., Buck, D. W., and Huttner, W. B. (2000) *J. Biol. Chem.* **275,** 5512–5520
8. Corbeil, D., Röper, K., Fargeas, C. A., Joester, A., and Huttner, W. B. (2001) *Traffic* **2,** 82–91
9. Corbeil, D., Röper, K., Weigmann, A., and Huttner, W. B. (1998) *Blood* **91,** 2625–2626
10. Miraglia, S., Godfrey, W., and Buck, D. (1998) *Blood* **91,** 4390–4391
11. Corbeil, D., Fargeas, C. A., and Huttner, W. B. (2001) *Biochem. Biophys. Res. Commun.* **285,** 939–944
12. Maw, M. A., Corbeil, D., Koch, J., Hellwig, A., Wilson-Wheeler, J. S. C., Bridges, R. J., Kumaramanickavel, G., John, S., Nancarrow, D., Röper, K., Weigmann, A., Huttner, W. B., and Denton, M. J. (2000) *Hum. Mol. Genet.* **9,** 27–34
13. Altschul, S. F., Madden, T. L., Schaffer, A. A., Zhang, J., Zhang, Z., Miller, W., and Lipman, D. J. (1997) *Nucleic Acids Res.* **25,** 3389–3402
14. Appel, R. D., Bairoch, A., and Hochstrasser, D. F. (1994) *Trends Biochem. Sci.* **19,** 258–260
15. Myers, E. W., and Miller, W. (1988) *Comp. Appl. Biosci.* **4,** 11–17
16. Thompson, J. D., Higgins, D. G., and Gibson, T. J. (1994) *Nucleic Acids Res.* **22,** 4673–4680
17. Felsenstein, J. (1989) *Cladistics* **5,** 164–166
18. Felsenstein, J. (1985) *Evolution* **39,** 783–791
19. Zhang, Q., Haleem, R., Cai, X., and Wang, Z. (2002) *Endocrinology* **143,** 4788–4796
20. Hurle, B., Lane, K., Kenney, J., Tarantino, L. M., Bucan, M., Brownstein, B. H., and Ornitz, D. M. (2001) *Genomics* **77,** 189–199
21. Yu, Y., Flint, A., Dvorin, E. L., and Bischoff, J. (2002) *J. Biol. Chem.* **277,** 20711–20716
22. Wilson, R., Ainscough, R., Anderson, K., Baynes, C., Berks, M., Bonfield, J., Burton, J., Connell, M., Copsey, T., and Cooper, J. (1994) *Nature* **368,** 32–38

[4] C. A. Fargeas, A. Joester, A. Hellwig, W. B. Huttner, and D. Corbeil, manuscript in preparation.

[5] A. Joester, C. Corbeil, C. A. Fargeas, A. Hellwig, and W. B. Huttner, manuscript in preparation.